ACS APPLIED MATERIALS & INTERFACES

RESEARCH ARTICLE

www.acsami.org

Facile Construction of Manganese Oxide Doped Carbon Nanotube Catalysts with High Activity for Oxygen Reduction Reaction and Investigations into the Origin of their Activity Enhancement

Zhi Yang,* Xuemei Zhou, Huagui Nie, Zhen Yao, and Shaoming Huang*

Nanomaterials and Chemistry Key Laboratory, Wenzhou University, Wenzhou 325027, China

ABSTRACT: MnOx-doped carbon nanotube (MnOx-CNTs) catalysts for the oxygen reduction reaction (ORR) were fabricated using a simple electrochemical deposition method. MnOx-CNTs (0.85 wt % MnOx) could exhibit an improved electrocatalytic activity, long-term stability and excellent resistance to crossover-effect compared to Pt/C catalysts. High-resolution transmission electron microscopy (HRTEM) and X-ray diffraction analysis confirm that the MnOx in the MnOx-CNTs exists in an amorphous state. Moreover, compared to the catalytic performances of MnOx on other substrates, the MnOx-CNTs exhibit a high ORR activity. X-ray photoelectron spectroscopy results suggest that the electron transfer, from the CNTs to the Mn ions occurs and the high positive charge is generated on the MnOx-CNT surface. This is believed to be origin of the catalytic activity observed in the ORR using MnOx-CNTs.

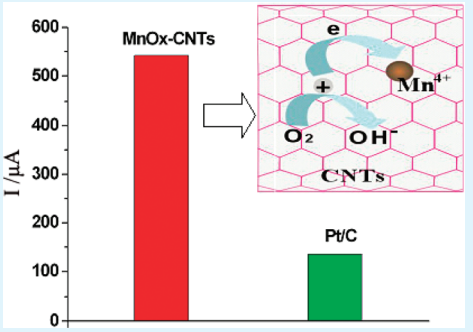

KEYWORDS: oxygen reduction, nitrogen-doped carbon nanotubes, manganese oxide, fuel cell

1. INTRODUCTION

The large-scale commercial application of fuel cells (FCs) has been hindered by the high cost and scarcity of the requisite noble metal materials.[1−3] The search for nonprecious-metal catalysts (NPMC), with both high activity and practical durability, has been viewed as a long-term strategy to promote the development of FCs.[4] Since Asinski et al.[5] observed that cobalt phthalocyanine could catalyze the oxygen reduction reaction (ORR), various NPMC materials,[5−9] including N-coordinated transition metal (TM) macromolecules, chalcogenides, oxynitrides, carbonitrides and TM-doped conductive polymers, have also been evaluated as potential substitutes for Pt-based catalysts. Nitrogen-doped carbon materials,[10−19] such as carbon nanotubes (CNT),[10−14] nanotube cups,[15] ordered mesoporous graphitic arrays,[16] and graphene,[17] have also attracted attention because of their excellent electrocatalytic activities. This has opened a way to prepare a new class of metal-free catalyst for the ORR. The doping of N atoms may result in the change to the CNTs' electronic structure, which could play a key role in their catalytic activity enhancement toward the ORR.[20,21] Dai et al.[10] proposed that the high activity may be attributed to the strong electronic affinity of N atoms and the substantial positive charge density on the adjacent C atoms. These factors may result in the very favorable adsorption of O_2. Some theoretical studies using simulation calculations also support this view.[22−24] More recently, Wang et al. found that CNTs functionalized with polyelectrolytes, which have a strong electron-withdrawing ability, may also act as efficient catalysts for the ORR.[25] However, direct experimental evidence to support this view is still pending.

Herein, we have developed a MnOx-doped CNT (MnOx-CNTs) catalyst for the ORR, prepared via a simple electrochemical deposition method. Although catalysts involving MnOx/C composites have been previously explored with respect to the ORR,[26−30] the carbon materials have generally acted as supports to improve the conduction and MnOx loading. In our work, we found that CNTs doped with a mere ∼0.85 wt % of MnOx, through electrochemical deposition, exhibit excellent electrocatalytic activity toward the ORR in an alkaline medium. The structure of the MnOx-CNTs was characterized through X-ray diffraction (XRD) and X-ray photoelectron spectroscopy (XPS) measurements. The catalytic performances of the pristine CNTs and MnOx on other substrates were assessed as control experiments. It is proposed that the high positive charge density on the doped CNTs plays a vital role in the excellent ORR activity. Our work, not only successfully develops an NPMC with excellent electrocatalytic activity, it also reveals further insight into the ORR mechanism of doped carbon materials.

2. EXPERIMENTAL SECTION

Electrode Preparation. Glassy carbon (GC) electrodes (3 mm diameter, CH instrument Inc.) were polished with a 0.05 and 0.3 μm alumina slurry (CH Instrument Inc.) on a microcloth, and subsequently rinsed with ultrapure water and ethanol. The electrodes were then sonicated in ultrapure water for 5 min to remove any bound particles, rinsed thoroughly with ultrapure water and dried under a gentle nitrogen stream. To prepare the working electrode, a 1 mg sample comprising CNTs, CB and KS-6 was ultrasonically dispersed in 1 mL of ethanol, and then 2 μL of the resulting suspension was dropped onto the GC surface

Received: April 7, 2011
Accepted: June 27, 2011
Published: June 27, 2011

Table 1. Specific Surface Areas for CNTs, CB, KS-6, MnOx-CNTs, MnOx-CB, and MnOx-KS-6

sample	deposition time (s)	MnOx content (wt %)	specific surface area (m^2/g)
CNTs	0	0	235.4
MnOx-CNTs	5	0.85	233.2
CB	0	0	201.7
MnOx-CB	5	0.80	205.3
KS-6	0	0	120.7
MnOx-KS-6	5	0.82	115.9

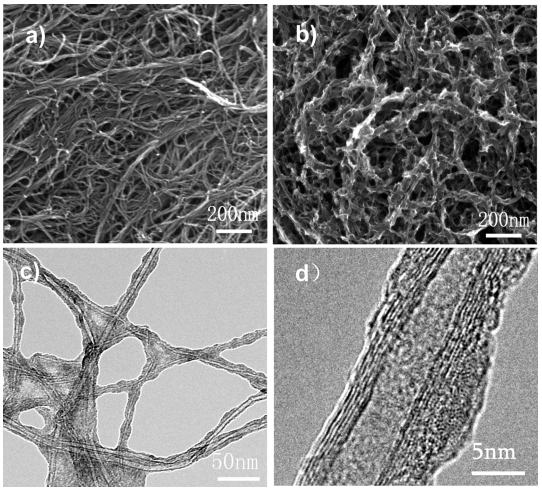

Figure 1. (a) SEM image of the pristine CNTs, and (b) SEM, (c) TEM and (d) HRTEM images of the MnOx-CNTs.

and dried at room temperature. For comparison, a commercially available Pt/C-modified GCE (20 wt % Pt supported on carbon black, fuel cell grade from Sigma) was prepared in the same way.

Synthesis of the MnOx-CNTs. MnOx-CNTs were synthesized using a facile electrochemical deposition method. In short, the CNT-modified electrodes were placed in 0.05 mM Na_2SO_4 solution containing 0.03 mM $MnSO_4$, and electrodeposited at an applied potential of +1.7 V under constant stirring. The MnOx mass content in the MnOx-CNTs was analyzed, through Inductively Coupled Plasma-Atom Emission Spectroscopy (ICP-AES), to be approximately 0.85 wt % after a deposition time of 5s. A MnOx-modified GCE, a MnOx-CB-modified GCE, and a MnOx-KS-6-modified GCE were all prepared in the same way. The MnOx mass contents for the MnOx/C composites were determined using ICP-AES. The specific surface areas of these samples were measured using the Brunauer–Emmett–Teller (BET) method. The physical parameters and corresponding experimental data are listed in Table 1.

Electrochemical Measurements. All electrochemical measurements, including cyclic voltammograms (CV), rotating-disk electrode voltammograms and chronoamperometry, were performed at room temperature in 0.1 M KOH solutions, which were purged with high purity nitrogen or oxygen for at least 30 min prior to each measurement. CV was performed within a potential range between −1.2 to +0.2 V, at a scan rate of 50 mV s^{-1}. Rotating-disk electrode voltammograms were recorded within a potential range between +0.2 to −1.0 V, at a scan rate of 10 mV s^{-1}. Chronoamperometry was performed at −0.35 V.

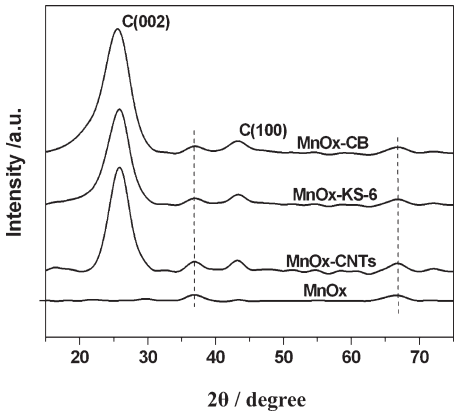

Figure 2. XRD curves for MnOx, MnOx-CNTs, MnOx-CB, and MnOx-KS-6.

3. RESULTS AND DISCUSSION

Figure.1 shows the SEM, TEM, and HRTEM images for the pristine CNTs and the MnOx-CNTs. It is clear from the SEM and TEM images in Figure 1a–c, that the surface of CNTs has been coated with MnOx. The HRTEM image in Figure 1d shows that MnOx coated on the surface of the CNTs is in the amorphous state. The XRD curves for the MnOx-CNTs in Figure.2 show two broad weak peaks at approximately 37 and 66°. The positions of these diffuse peaks are similar to those reported for amorphous manganese oxides.[31−33] The XRD results confirm the presence of amorphous manganese oxides in the MnOx-CNTs, and are also consistent with HRTEM observations.

To investigate the electrocatalytic activity of the MnOx-CNTs, we measured the cyclic voltammograms (CVs) for the MnOx-CNTs and the commercial Pt/C (20 wt % Pt on Vulcan XC-72) in 0.1 M KOH solutions, saturated with N_2 or O_2. Equal amounts of each catalyst (28.2 μg cm^{-2}) were loaded on a glassy-carbon electrode. As shown in Figure 3a, the CV curve for MnOx-CNT electrode in O_2 shows a distinct peak at −0.35 V, which corresponds to the O_2 reduction reaction. The reduction current (542 μA, Figure 3a) is more than four times larger than that of the commercial Pt/C catalyst (135 μA, Figure 3b). The polarization curves in Figure.3c show that MnOx-CNTs have more positive onset potentials and a higher limiting current than the commercial Pt/C catalysts. These results suggest that MnOx-CNTs have a more pronounced catalytic activity for the ORR than commercial Pt/C catalysts.

The stability and the possible crossover effects of the catalyst materials are important considerations for their practical application to fuel cells. Therefore, the electrocatalytic selectivity of the MnOx-CNTs against the electrooxidation of methanol was measured. In Figure 3a, after the addition of 3 M methanol to a 0.1 M KOH solution saturated with O_2, no noticeable change is observed for the oxygen-reduction current at the MnOx-CNTs electrode. This indicates that MnOx-CNTs exhibit a high selectivity for the ORR with a remarkably good ability to avoid crossover effects. The durability of the MnOx-CNTs and the commercial Pt/C catalyst were also tested. The catalysts were held at −0.35 V for more than 10,000s in an O_2 saturated 0.1 M KOH solution, at a stir rate of 1600 rpm. From Figure 3d, the chronoamperometric response for the MnOx-CNTs exhibits a very slow attenuation within the first 2000 s,

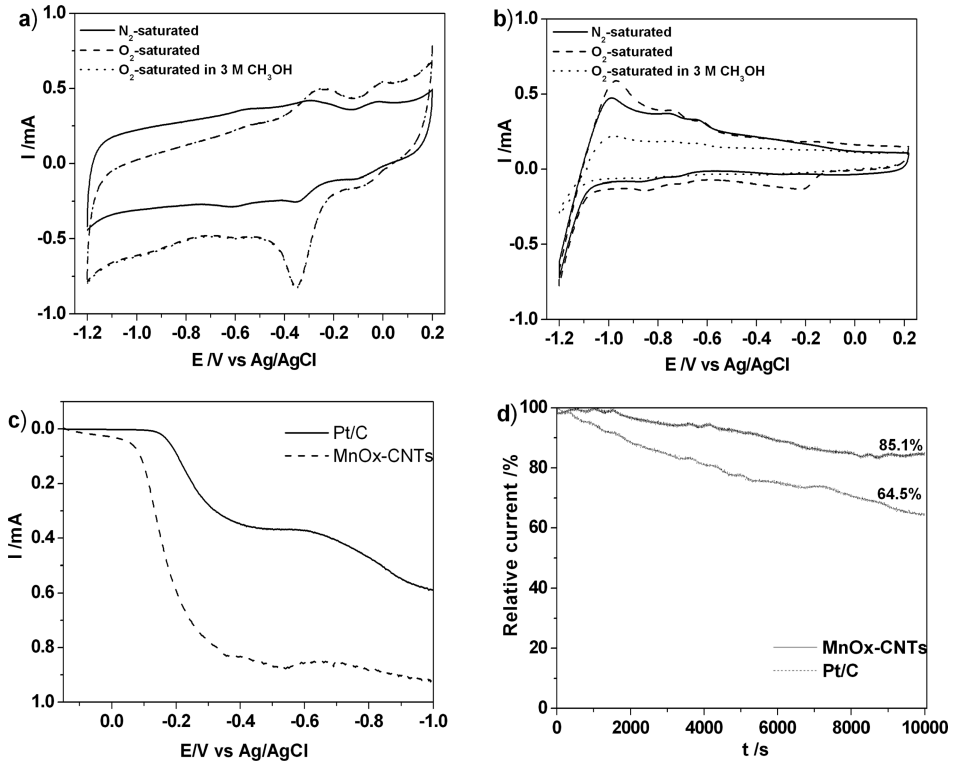

Figure 3. Cyclic voltammograms of (a) MnOx-CNTs and (b) the commercial Pt/C catalyst, for the oxygen reduction reaction in 0.1 M KOH solutions saturated with N_2 or O_2. (c) Polarization curves for the MnOx-CNTs and the Pt/C catalyst on a glass carbon rotating disk electrode, in a saturated O_2 at a rotation rate of 1600 rpm (d) Current−time (i−t) chronoamperometric response of the MnOx-CNTs and the Pt/C-modified GC electrodes at −0.35 V, in an O_2-saturated 0.1 m KOH at a rotation rate of 1600 rpm.

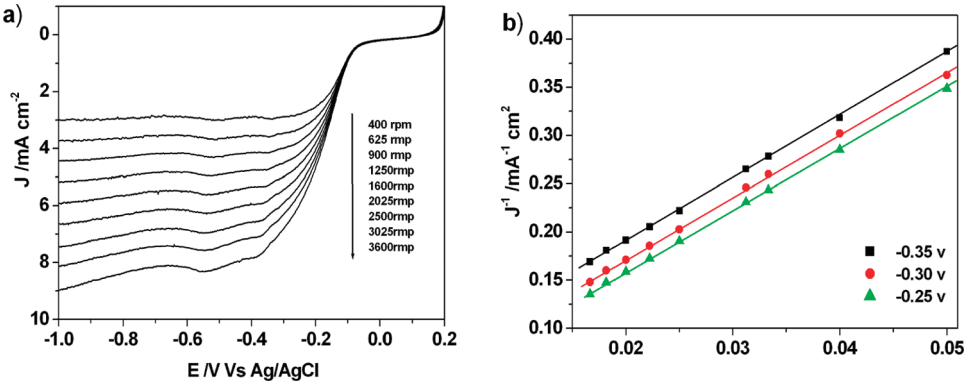

Figure 4. (a) Rotating-disk voltammograms recorded for the MnOx-CNT electrode in an O_2-saturated 0.1 M KOH solution at different rotation rates. (b) Koutecky−Levich plot of J^{-1} versus $\omega^{-1/2}$, at different electrode potentials. The experimental data were obtained from Figure 4a and the lines are linear regressions.

and a high relative current of 85.1% after 10 000 s. In contrast, the Pt/C electrode exhibits a gradual decrease, with a current loss of approximately 64.5% after 10 000 s. These results confirm that MnOx-CNTs have a potential use in direct methanol and alkaline fuel cells.

To further study the ORR procedures with respect to MnOx-CNTs, we performed rotating-disk electrode (RDE) experiments. The RDE current−potential curves, at various rotating speeds, are shown in Figure 4. The limited diffusion currents are dependent on the rotation rates. The number of electrons involved in the ORR can be calculated from the Koutecky−Levich (K−L) equation

$$J^{-1} = J_L^{-1} + J_K^{-1} = (B\omega^{1/2})^{-1} + J_K^{-1} \quad (1)$$

$$B = 0.62nFC_0(D_0)^{2/3}\nu^{-1/6} \quad (2)$$

Where J is the measured current density, J_K and J_L are the kinetic- and diffusion-limiting current densities, ω is the angular velocity of the disk ($\omega = 2pN$, N is the linear rotation speed), n is the overall number of electrons transferred in the oxygen reduction, F is the Faraday constant ($F = 96485$ C mol^{-1}), C_0 is

dx.doi.org/10.1021/am200426q |ACS Appl. Mater. Interfaces 2011, 3, 2601–2606

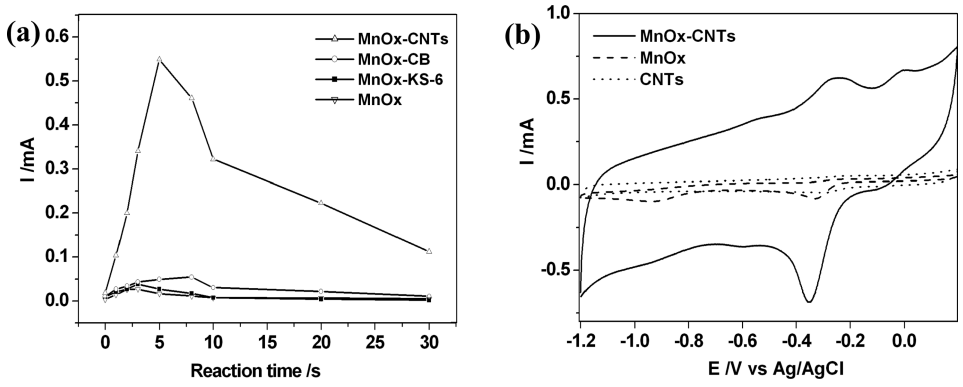

Figure 5. (a) Reduction current versus reaction time for MnOx on four different substrates, (b) Cyclic voltammograms of the pristine CNTs, the MnOx sample after a deposition time of 3s and the MnOx-CNTs, for the oxygen reduction reaction in a 0.1 M KOH solution saturated with O_2.

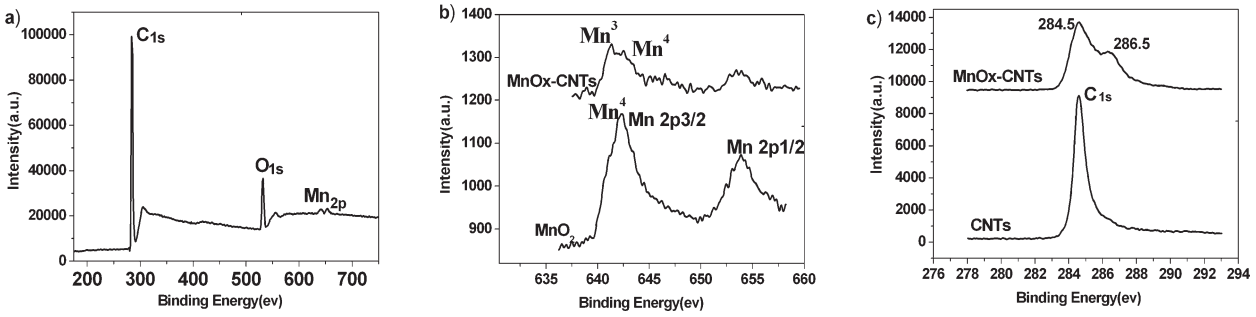

Figure 6. (a) XPS spectra survey scan, high-resolution (b, upper) Mn_{2p} and (c, upper) C_{1S} for the Mn-doped CNTs, (b, bottom) Mn_{2p} of MnO_2 and (c, bottom) C_{1S} of pristine CNTs.

the bulk concentration of O_2 ($C_0 = 1.2 \times 10^{-6}$ mol cm^{-1}), ν is the kinematic viscosity of the electrolyte ($\nu = 0.01$ cm^2 s^{-1}), and D_0 is the diffusion coefficient of O_2 in 0.1 M KOH (1.9×10^{-5} cm^2 s^{-1}). According to eqs 1 and 2, the number of electrons transferred (n) can be calculated to be 3.9 at −0.35 V, which suggests the MnOx-CNTs lead to a four-electron-transfer reaction, reducing oxygen to OH^-. The above-described results suggest that the MnOx-CNTs are a promising NPMC with a high catalytic activity for the ORR.

A number of MnO_2/C composites have been reported to exhibit specific activities for the ORR similar to the benchmark Pt/C catalyst.[26,27] However, such excellent activity for ORR based on the MnOx-CNTs (0.85 wt % MnOx) has been rarely reported. To investigate the key factors that lead to the catalytic activities for the MnOx-CNTs, a range of experiments have been performed. The XRD curves in Figure 2 indicate that all the deposited MnOx, on all the different substrates, is in an amorphous state. BET measurements (Table 1) also show that the specific surface area values for these C materials do not change significantly after a deposition time of 5 s. Therefore, the effects of MnOx structure and specific surface area on the catalytic activity can be eliminated in our experiments. The curve for MnOx-CNT reduction current as a function of reaction time, as shown in Figure 5a, displays a volcano-like shape, with an initial increase in ORR current. After a deposition time of 5 s (0.85 wt % MnOx), the MnOx-CNTs exhibited the maximum ORR current. Their current then decreases with MnOx content, when the deposition time is taken beyond 5 s. This may be due to the comparatively high MnOx content, and may result in a decrease

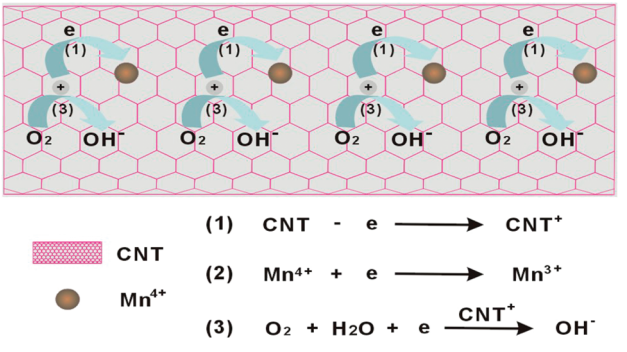

Figure 7. Schematic diagram for the MnOx-CNT ORR mechanism.

in the interface area between the CNTs and the electrolyte, which would increase the resistance for the MnOx-CNT electrode. For other MnOx samples on different substrates, a similar tendency is observed. For example, a MnOx sample after a deposition time of 3 s exhibits the highest ORR activity of all the MnOx samples on a bare glassy carbon electrode. However, the reduction current (27.2 μA) is still lower than that for the MnOx-CNTs (542 μA). Figure 5b shows the CV curves for the pristine CNTs, the MnOx sample after a deposition time of 3 s and the MnOx-CNTs (0.85 wt % MnOx) from the ORR. From Figures 5a,b, the MnOx-CNTs exhibit a remarkably high catalytic activity compared to the other materials. Their maximum current (542 μA) is 50 times higher than that of the pristine CNTs (10.2 μA), and more than 10 times larger than that of the other MnOx

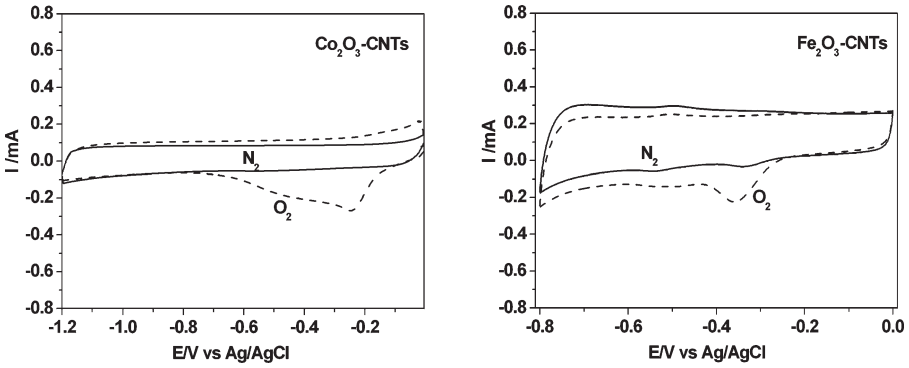

Figure 8. Cyclic voltammograms for the Co_2O_3−CNTs and Fe_2O_3−CNTs, for the oxygen reduction reaction in 0.1 M KOH solutions saturated with N_2 or O_2.

samples on different substrates (49.3, 27.7, and 27.2 μA for MnOx-CB, MnOx-KS-6, and MnOx, respectively). All these results confirm that the CNTs play a key role in the excellent ORR activity. Considering the very low MnOx content (a mere 0.85 wt %) and the low catalytic activity for the other MnOx samples on different substrates, we propose that the catalytic activity originating from the MnOx within the CNTs is limited. Thus, the traditional view, where the MnOx bears the active site for the ORR and carbon materials act only as a support, can not explain our observations herein. The unique electron structure of the doped MnOx-CNTs may play a vital role in the observed ORR activity enhancement, and the doped CNTs may be the actual host for catalyzing the ORR.

The origin of this ORR activity enhancement with the N-doped CNTs has been previously explored. According to Dai and Hu, based on theoretical calculations,[10,22] the build up in positive charge on CNT surfaces would establish favorable sites for the side-on O_2 surface adsorption. This parallel diatomic adsorption could effectively weaken the O−O bonding and facilitate the direct reduction of oxygen to OH^- via a four-electron process. The redox potential for the CNTs is about +0.5 V, vs the standard hydrogen electrode (SHE),[34] and the reduction potential for MnO_2 (MnO_2/Mn^{3+}) is +0.95 V (vs SHE), which would lead to a spontaneous electron transfer from the nanotube to the MnO_2. Similar observations have been previously reported[34−36] involving other metal ions and CNTs, such as $AuCl^{4-}$ and single-walled carbon nanotubes. We propose that the spontaneous electron transfer between CNTs and MnO_2 will result in the high positive charge on the CNT surface, which may facilitate the ORR activity enhancement. To interrogate the electronic structure of the MnOx-CNT surface, we measured the XPS spectrum. The XPS survey spectrum in Figure 6a reveals a predominant C_{1s} peak (284.5 eV), an O_{1s} peak (532.0 eV) and two Mn_{2p} peaks (641.4 eV, 653.9 eV), which further suggest that the MnOx is formed on the MnOx-CNT composites. The chemical states of Mn and C in the MnOx-CNTs were analyzed using XPS high-resolution C_{1s} and Mn_{2p} spectra, as shown in Figure 6b and c. Upon comparing the Mn_{2p} peaks for MnO_2 (Figure 6b, bottom), the $Mn_{2p3/2}$ appears as two peaks, at 641.4 and 642.3 eV, for the MnOx-CNTs, which may be attributed to Mn^{3+} and Mn^{4+}, respectively.[37] For the C_{1s} spectra, a new peak is observed at 286.5 eV (Figure 6c upper) for the MnOx-CNTs, in addition to the predominant peak at 284.5 eV observed in the pristine CNT spectra (Figure 6c bottom). These results are strongly consistent with an electron transfer between the CNTs and the Mn ions, which results in a high positive charge on the MnOx-doped CNTs. A Schematic diagram for the electron transfer is depicted in Figure 7. The electronic structure characteristic of the MnOx-CNTs, with the high catalytic activity, is very similar to the structure model proposed by Dai et al. for N-doped CNTs. The above-described RDE result also confirms that the MnOx-CNTs undergo a four-electron-transfer ORR process, consistent with that observed for the N-doped CNTs. These results further suggest that nitrogen and MnOx-doped CNTs operate via the same activity-enhancement mechanism and the resultant high positive charge density on the doped CNT surface may lead to the activity enhancement for the ORR.

On the basis of this understanding, we further speculated that CNTs doped with other metal oxides may exhibit a similarly high catalytic activity for the ORR. We prepared CNTs doped with Co_2O_3 (Co^{3+}/Co^{2+}, +1.84 v vs SHE) and Fe_2O_3 (Fe^{3+}/Fe^{2+}, +0.77 v vs SHE), and as expected, both exhibited a higher catalytic activity for the ORR than the commercial Pt/C catalyst (Figure 8). These results further emphasize the importance of the build up in positive charge density on the doped CNTs for catalytic activity.

4. CONCLUSIONS

In summary, we have reported a MnOx-CNT ORR catalyst, fabricated through a simple electrochemical deposition method, which boasts a greater electrocatalytic activity than current commercial Pt/C catalysts. They also exhibit long-term stability and an excellent resistance to crossover effects for the ORR. Moreover, our results confirm that the electron transfer from the CNTs to the Mn ions occurs, which generates the high positive charge on the MnOx-CNT surface. This is believed to be the origin of the MnOx-CNT catalytic activity enhancement for the ORR. These results could provide useful information to further clarify the ORR mechanism of doped carbon materials, and further develop other novel low-cost NPMCs with high activities and long lifetimes for practical FC application.

AUTHOR INFORMATION

Corresponding Author

*E-mail: smhuang@wzu.edu.cn (S.H.), yang201079@126.com (Z.Y.).

ACKNOWLEDGMENT

The work was supported in part by grants from NSFC (51002106, 21005055) and NSFC for Distinguished Young

Scholars (51025207), BSTWZ (G20100191), NSFZJ (R4090137, Y4100520), and ZJED Innovative Team for S. Huang.

REFERENCES

(1) Winter, M.; Brodd, R. J. *Chem. Rev.* **2004**, *104*, 4245–4270.
(2) Chen, Z. W.; Waje, M.; Li, W. Z.; Yan, Y. S. *Angew. Chem.* **2007**, *119*, 4138–4141.
(3) Lim, B.; Jiang, M. J. P.; Cho, E. C.; Tao, J.; Lu, X. M.; Zhu, Y. M.; Xia, Y. N. *Science* **2009**, *324*, 1302–1305.
(4) Serov, A.; Kwak, C. *Appl. Catal., B* **2009**, *90*, 313–320.
(5) Jasinski, R. *Nature* **1964**, *201*, 1212–1213.
(6) Bashyam, R.; Zelenay, P. *Nature* **2006**, *443*, 63–66.
(7) Gong, K.; Yu, P.; Su, L.; Xiong, S.; Mao, L. *J. Phys. Chem. C* **2007**, *111*, 1882–1887.
(8) Collman, J. P.; Devaj, N. K.; Decreau, R. A.; Yang, Y.; Yan, Y. L.; Ebina, W.; Eberspacher, T. A.; Chidsey, C. E. D. *Science* **2007**, *315*, 1565–1568.
(9) Winther-Jensen, B.; Winther-Jensen, O.; Forsyth, M.; MacFarlane, D. R. *Science* **2008**, *321*, 671–674.
(10) Gong, K. P.; Du, F.; Xia, Z. H.; Durstock, M.; Dai, L. M. *Science* **2009**, *323*, 760–764.
(11) Xiong, W.; Du, F.; Liu, Y.; Perez, A.; Supp, M.; Ramakrishnan, T. S.; Dai, L. M.; Jiang, L. *J. Am. Chem. Soc.* **2010**, *132*, 15839–15841.
(12) Yu, S. S.; Zhang, Q.; Dai, L. M. *J. Am. Chem. Soc.* **2010**, *132*, 15127–15129.
(13) Wang, Z. J.; Jia, R. R.; Zheng, J. F.; Zhao, J. H.; Li, L.; Song, J. L.; Zhu, Z. P. *ACS Nano* **2011**, *5*, 1677–1684.
(14) Nagaiah, T. C.; Kundu, S.; Bron, M.; Muhler, M.; Schuhmann, W. *Electrochem. Commun.* **2010**, *12*, 338–341.
(15) Tang, Y. F.; Allen, B. L.; Kauffman, D. R.; Star, A. *J. Am. Chem. Soc.* **2009**, *131*, 13200–13201.
(16) Liu, R. L.; Wu, D. Q.; Feng, X. L.; Mullen, K. *Angew. Chem.* **2010**, *49*, 2565–2569.
(17) Qu, L. T.; Liu, Y.; Baek, J. B.; Dai, L. M. *ACS Nano* **2010**, *4*, 1321–13236.
(18) Shanmugam, S.; Osaka, T. *Chem. Commun.* **2011**, *47*, 4463–4465.
(19) Yang, W.; Fellinger, T. P.; Antonietti, M. *J. Am. Chem. Soc.* **2011**, *133*, 206–209.
(20) Kurak, K. A.; Anderson, A. B. *J. Phys. Chem. C* **2009**, *113*, 6730–6734.
(21) Sidik, R. A.; Anderson, A. B.; Subramanian, N. P.; Kumaraguru, S. P.; Popov, B. N. *J. Phys. Chem. B* **2006**, *110*, 1787–1793.
(22) Hu, X. B.; Wu, Y. T.; Li, H. R.; Zhang, Z. B. J. *J. Phys. Chem. C* **2010**, *114*, 9603–9607.
(23) Shan, B.; Cho, K. *Chem. Phys. Lett.* **2010**, *492*, 131–136.
(24) Yang, S. Z; Zhao, G. L.; Khosravi, E. *J. Phys. Chem. C* **2010**, *114*, 3371–3375.
(25) Wang, S. Y.; Yu, D. S.; Dai, L. M. *J. Am. Chem. Soc.* **2011**, *133*, 5182.
(26) Cheng, F. Y.; Su, Y.; Liang, J.; Tao, Z. L.; Chen, J. *Chem. Mater.* **2010**, *22*, 898–905.
(27) Cheng, F. Y.; Shen, J.; Peng, Mao.; Pan, Y. D.; Tao, Z. L.; Chen, J. *Nature Chem.* **2011**, *3*, 79.
(28) Verma, A.; Jha, A. K.; Basu, S. *J. Power. Sources* **2005**, *141*, 30–34.
(29) Chainet, I. R.; Chatenet, M.; Vondr_ak, J. *J. Phys. Chem.C.* **2007**, *111*, 1434–1443.
(30) Wang, Y. G.; Cheng, L.; Li, F.; Xiong, H. M.; Xia, Y. Y. *Chem. Mater.* **2007**, *19*, 2095–2101.
(31) Yang, J. S.; Xu, J. J. *J. Power Sources* **2003**, *122*, 181.
(32) Kawaoka, H.; Hibino, M.; Zhou, H.; Honma, I. *J. Power Sources* **2004**, *125*, 89.
(33) Kim, J.; Manthiram, A. *Nature* **1997**, *390*, 265.
(34) Choi, H. C.; Shim, M.; Bangsaruntip, S.; Dai, H. J. *J. Am. Chem. Soc.* **2002**, *124*, 9058–9095.
(35) Qu, L. T.; Dai, L. M. *J. Am. Chem. Soc.* **2005**, *127*, 10806–108067.
(36) Chen, W.; Fan, Z. L.; Pan, X. L.; Bao, X. H. *J. Am. Chem. Soc.* **2008**, *130*, 9414–9419.
(37) Mei, Y.; Chen, L.; Cao, Y. Z.; Liu, B. Q.; He, J. H.; Zhu, Z. W.; Xu, Z. A. *Acta Phys. Sin.* **2010**, *59*, 2795.